http://journal.uir.ac.id/index.php/JGEET

E-ISSN : 2541-5794
P-ISSN : 2503-216X

Journal of Geoscience,
Engineering, Environment, and Technology
Vol 11 No 1 2026

RESEARCH ARTICLE

Optimization of Coastline Extraction Using MNDWI Thresholds and Machine Learning on Landsat Images of Wetlands in Northern East Java, Indonesia

Shofura Afanin Nuha[1,*], Nurul Khakhim[1], Pramaditya Wicaksono[1]

[1] *Departement Remote Sensing, Faculty of Geography, Universitas Gadjah Mada, Yogyakarta 55281, Indonesia*

* Corresponding author : Shofura.afanin.nuha@gmail.com
Tel.:+62-858-5466-5053
Received: July 1, 2026; Accepted: Nov 20, 2016.
DOI: 10.24273/jgeet.2016.1.2.001

Abstract

This study evaluates and compares methods for extracting coastlines in the wetland coastal areas of northern East Java, specifically in Sidoarjo and Gresik Regencies, East Java, Indonesia. By analyzing eight scenarios that integrate bands from Landsat 8 imagery, the Modified Normalized Difference Water Index (MNDWI), and the SRTM Digital Elevation Model (DEM) under two machine learning classifiers (Random Forest and Classification and Regression Trees) on the Google Earth Engine (GEE) platform. Using a dataset consisting of 180 ground-truth points, we found that Random Forest (RF) combined with MNDWI and DEM (Scenario 5) achieved the highest overall accuracy (OA = 76%, Kappa = 0.71) in the flat wetlands of Sidoarjo, which are dominated by aquaculture ponds and mangrove vegetation. In contrast to the diverse Gresik coastal area, where some regions are dominated by industry, the pure CART model (Scenario 6) yielded the best results (OA = 66%, Kappa = 0.60), as the addition of DEM and MNDWI caused overfitting due to extreme local spectral and vertical disturbances from the complex coastal structure. These results indicate that ensemble-based classification (RF) with elevation filtering is crucial for distinguishing the microtopography of aquaculture ponds from natural seawater, whereas a single decision tree (CART) performs better with raw spectral inputs in structurally heterogeneous coastal environments.

Keywords: Coastlines, MNDWI, Random Forest, CART, Landsat, Wetlands

1. Introduction

Coastlines undergo continuous changes caused by erosion and accretion (Mentaschi et al., 2018), each of which has its own impact both beneficial and detrimental on the surrounding coastal areas (Marfai et al., 2013). Coastline changes are highly dynamic and natural, influenced by waves, wind, water flow, sea-level rise, and sediment transport (Li et al., 2023). However, human activities and the environmental impacts of global warming are amplifying these changes (Liang et al., 2025). Global warming leads to a rise in average sea levels, which has the potential to affect coastlines (Arjasakusuma et al., 2021).

Coastal erosion, such as land subsidence and erosion around the coast, can also be influenced by extreme weather conditions and coastal morphodynamics specifically, increasingly strong winds, waves, and atmospheric pressure (Pattipawaej and Oktaviani, 2023).On the other hand, accretion, or the addition of land, is caused by sediment flowing from upstream to downstream rivers due to human activities such as aquaculture, some of which are beneficial. Coastal dynamics are highly complex (Ondara et al., 2020); accretion the accumulation of sediment can occur, as can erosion that removes sediment through ocean waves and tidal currents (Costa Santos et al., 2019)

These highly dynamic and complex physical processes require specialized and continuous monitoring to track changes in land loss or gain over specific periods or years (Faiez and Fan, 2023). By leveraging remote sensing technology, tracking these rapid physical shifts becomes significantly more efficient, thereby enabling precise multi-temporal mapping of coastlines changes .

In this study, remote sensing is used to monitor the coastlines by extracting a boundary line between land and water known as the coastlines (Lou et al., 2024). Remote sensing that using with Radiometri, Geometric Corrections and Composite Image in the Landsat image dataset used to extraction techniques (Amukti et al., 2020). However, errors may occur in extracting the coastlines due to pixels or algorithms that cannot distinguish between land and water (Adeli et al., 2025), for example in wetland areas such as fish ponds, river estuaries, and mangrove vegetation areas (Muhammad Usman Zakaria et al., 2025). This study focuses specifically on the coastlines directly associated with coastal areas in northern East Java, which features a coastal type characterized by wetland areas. In this region, there are numerous active fish ponds used by local residents to boost the economy through natural aquaculture, as well as mangrove vegetation in several areas. This enables the monitoring of coastlines changes, particularly regarding land use and environmental management especially in wetlands using more efficient and rapid remote sensing methods (Halim, 2016).

Remote sensing provides data for analyzing the temporal dynamics of coastlines (Sadewa and Supriyadi, 2024). Methods such as Threshold, which applies a threshold value to the results of satellite image band/channel transformations to limit or separate desired objects based on their pixel values (Xu, 2006), and machine learning methods (Tyralis et al., 2019) that allow for tuning and adjusting the number of decision trees such as Random Forest (RF) (Çelik and Gazioğlu, 2022) and Classification and Regression Tree (CART) enable the distinction between water and land objects (Eteh et al., 2024). The more data integrated with remote sensing and GIS, the higher the accuracy of predictions regarding the extraction model and changes in the coastline (Hariyanto et al., 2018).

2. Methodology

2.1. Study Area

This study covers the coastal wetland areas of Sidoarjo and Gresik Regencies in East Java Province, Indonesia. The Sidoarjo coast is characterized by a very flat topography, dominated by the Porong River estuary, mangrove vegetation, and extensive aquaculture ponds (Arifianto and Wibowo, 2020). On the other hand, the coast of Gresik Regency, in addition to having the active Bengawan Solo delta in Ujung Pangkah District and aquaculture areas, has undergone intensive anthropogenic modification due to the development of heavy industrial zones, including the Java Integrated Industrial and Ports Estate (JIIPE) port; therefore, coastlines extraction is necessary to observe the development of its coastal dynamics. The extraction must use a method that is unique and appropriate for the studied area. Figure 1 shows the map of the study area.

There are two regencies Gresik Regency and Sidoarjo Regency to the east specifically to the south across the Madura Strait which has experienced significant sediment transport (Murray et al., 2022) following the 2006 Lapindo mudflow gas leak. To address these complex coastal dynamics (Barbier et al., 2011), this study evaluates and compares various digital coastline extraction methods. The entire computational analysis and model optimization are executed cloud-basiately on the Google Earth Engine (GEE) platform.

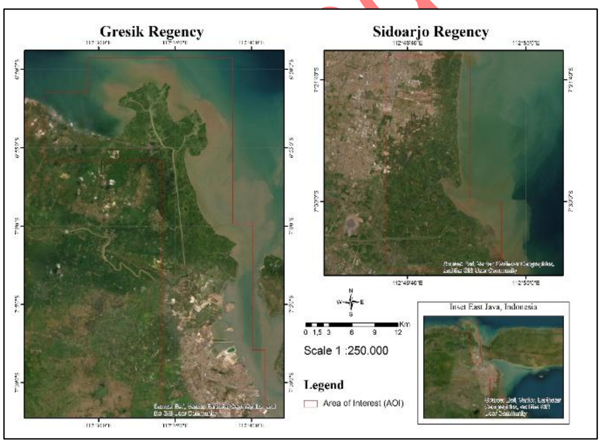

Fig. 1 Study Area Gresik and Sidoarjo Regency

2.2. Data and Preprocessing

This study uses Landsat 8 Operational Land Imager (OLI) Surface Reflectance (SR) Tier 1 satellite imagery recorded on August 14, 2025. The recording time was selected during the local low tide to ensure maximum exposure of the intertidal zone boundaries. Elevation data from the Shuttle Radar Topography Mission (SRTM) 1 Arc-Second Global DEM (30-meter resolution) were integrated to provide vertical topographic boundaries. Training and validation samples were collected using a stratified random sampling design, resulting in a total of 180 sample points (70% used as training data and 30% for independent validation) distributed across six macro-land cover classes: Open Water, Open Land, River Water, Vegetation, Aquaculture Ponds, and Built-up Land (Congalton and Green, 2008). Data availability and sources are shown in Table 1 below.

Table 1. Research Data Requirements

Data	Data Sources
Coastline and Land Use Validation Based on the location points created, specifically field data from 2026	Field survey using GPS Essentials
Landsat 8 OLI TIRS imagery from 2025 for coastline extraction comparison	Google Earth Engine, USGS (https://earthexplorer.usgs.gov/)
SRTM DEM for PL validation with slope boundaries and data output/integration together with MNDWI	Google Earth Engine, USGS (https://earthexplorer.usgs.gov/)

2.3. Experimental Design

Eight classification scenarios were designed and run on GEE to extract the water-land binary boundary between the Random Forest (RF) and Classification and Regression Tree (CART) algorithms, as well as using the MNDWI index and SRTM DEM.

Table 2. The Scenario Used in the Study

Scenario	Description	Band
1	MNDWI	NIR + SWIR1
2	MNDWI + DEM	NIR + SWIR1 + Elev
3	RF	RGB, NIR, SWIR 1, SWIR2
4	RF + MNDWI	RGB, NIR, SWIR 1, SWIR2, MNDWI
5	RF MNDWI DEM	RGB, NIR, SWIR 1, SWIR2, MNDWI + Elev
6	CART	RGB, NIR, SWIR 1, SWIR2
7	CART + MNDWI	RGB, NIR, SWIR 1, SWIR2, MNDWI
8	CART MNDWI DEM	RGB, NIR, SWIR 1, SWIR2, MNDWI + Elev

To generate a clean seawater boundary, the multi-class classification results from the best-case scenario were converted into a binary map (Seawater vs. Land/Other Water Bodies). The Canny Edge Detector algorithm was then applied to the GEE to convert this binary boundary into a vector coastline in ArcGIS software, thereby generating the 2025 coastline boundary.

3. Results and Discussion

3.1 Extraction with Index MNDWI

A method for extracting coastlines that utilizes differences in spectral reflectance characteristics between water bodies and land in the electromagnetic spectrum by using indices in existing bands or channels (Simarmata et al., n.d.). Water exhibits very strong absorption in the near-infrared (NIR) and shortwave infrared (SWIR) bands, while land objects such as vegetation, soil, and built-up areas reflect significantly more energy in these bands. To mitigate the negative effects of urban features and open land—which often cause classification errors in the standard Normalized Difference Water Index (NDWI)—the Modified Normalized Difference Water Index (MNDWI) was implemented by replacing the NIR band with the SWIR band (Syamani, 2021). The mathematical formulation of the MNDWI is defined in Eqn. (1) as follows:

$$MNDWI = \frac{Green - SWIR1}{Green + SWIR1} \quad (1)$$

To automatically separate pixels of pure seawater (class 1) and non-water (classes 2–6) from MNDWI raster images, a manual threshold segmentation algorithm was applied, which involved identifying threshold values that corresponded to the visual appearance of the image. The values obtained from several trials, ranging from thresholds of 0.0 to 0.6, demonstrate that a threshold of 0.0 is sufficient to optimize the boundary between water and land, as well as to minimize errors in the cloud coverage present in the Landsat satellite imagery. The differences in threshold results for MNDWI can be seen in Table 3 below:

Table 3. Threshold for MNDWI

Threshold Input	MNDWI Result
0.0	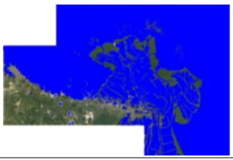
0.10	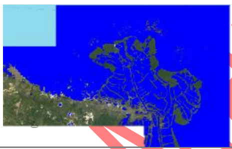
0.20	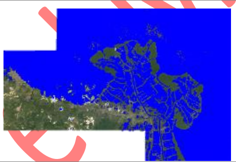
0.30	
0.40	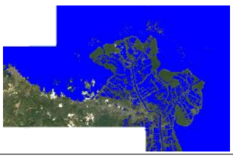
0.50	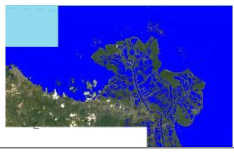
0.60	

The results of Canny edge detection or boundary line extraction on MNDWI using DEM, as presented in Table 4, demonstrate a difference between using MNDWI alone (Scenario 1) and adding DEM (Scenario 2). By using the SRTM DEM directly, it is possible to distinguish between inland water and seawater; however, overclassification still occurs because the DEM input often classifies additional areas in the coastal region as seawater, specifically in Gresik Regency.

Table 4. Extraction Result MNDWI & DEM Gresik Regency

Landsat 2025 Imagery	MNDWI	MNDWI DEM
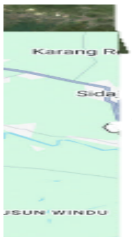		
Extraction Results for Gresik Regency	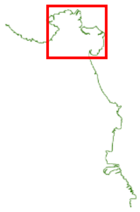	

Meanwhile, in Sidoarjo Regency, specifically at the mouth of the Porong River, the MNDWI results are more sensitive to the river mouth, causing the coastline to extend into the river area. However, MNDWI alone is capable of mapping or extracting Lusi Island, which is located at the mouth of the Porong River. The image is presented in Table 5 below.

Table 5. Extraction Result MNDWI & DEM Sidoarjo Regency

Landsat 2025 Imagery	MNDWI	MNDWI DEM
		
Extraction Results for Sidoarjo Regency		

3.2 Extraction with RF

The results of the RF scenario coastline extraction in Gresik Regency were quite satisfactory, as they successfully produced a well-defined coastline at the end of the data processing (Aslam et al., 2024). These results have been optimized using a threshold with the highest hyperparameter tuning settings, namely *numTrees* set to 100 and *minLeafRF* set to 1.

Table 6. Extraction Result Random Forest Gresik Regency

Classification RF	RF + MNDWI	RF MNDWI DEM

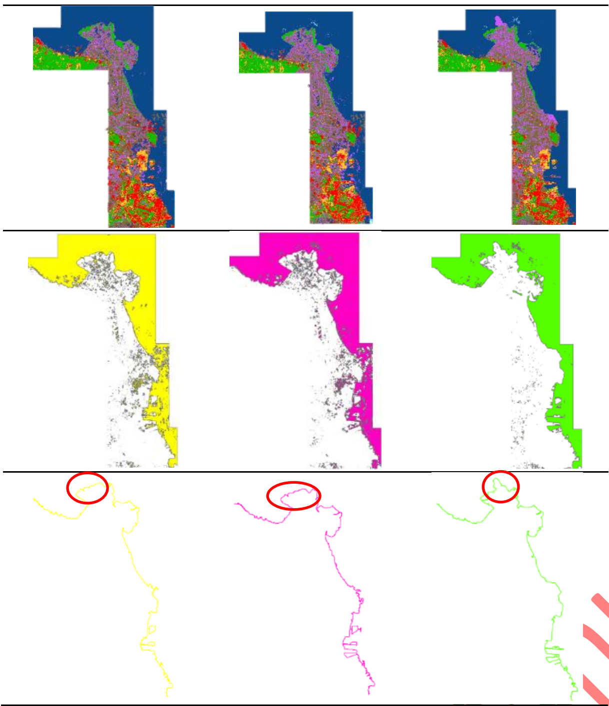

Table 7. Extraction Result Random Forest Sidoarjo Regency

Classification RF	RF + MNDWI	RF MNDWI DEM

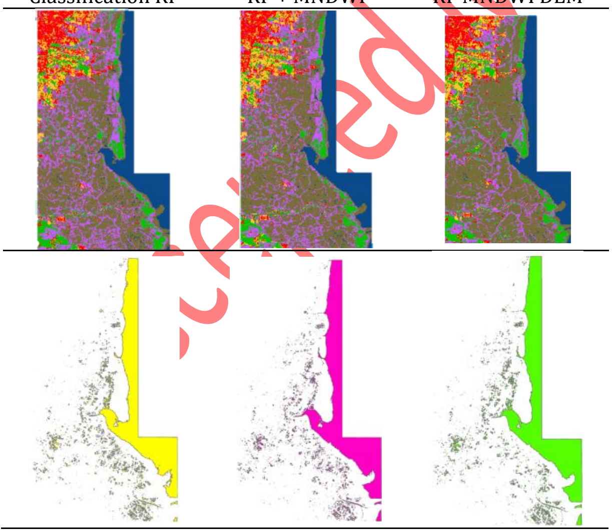

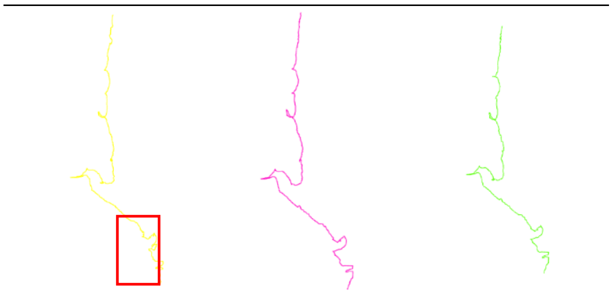

The comparison results of the scenarios using Random Forest specifically scenarios 3, 4, and 5 show significant differences, as shown in Table 6. The classification results for Scenario 5, which uses MNDWI and DEM, are overestimated at the northernmost tip of the peninsula, as indicated by the red circle. This is caused by sediment shadows in the imagery, which allow the coastline to be drawn in that area. The line extends too far out to sea, exceeding the actual conditions on the ground. This anomaly indicates an overestimation of the land area.

The RF results for overall accuracy in Sidoarjo Regency showed the highest value, with an OA of 76% and a Kappa of 0.71, which will be discussed in the chapter on the best extraction results. This demonstrates that RF can be effectively applied to coastal typologies such as those in Sidoarjo Regency, which features wetland typologies characterized by aquaculture ponds and mangrove vegetation . The extraction results between scenarios 3, 4, and 5 show slight differences; specifically, scenario 3 (pure RF) exhibits discrepancies in the coastline for the fish ponds. However, this can be addressed by incorporating MNDWI and DEM in scenarios 4 and 5, though the results remain imperfect due to overestimation errors occurring at the Porong River Estuary, as indicated by the red box in Table 7.

3.3 Extraction with CART

The resulting CART machine learning model is the outcome of different hyperparameter tuning optimizations between Gresik Regency with nodeLimit set to 100 and minLeafCART to 5, yielding an accuracy of 66% and Sidoarjo Regency with nodeLimit set to 100 and minLeafCART to 1, yielding an accuracy of 74%. In Gresik Regency, the highest accuracy was achieved in Scenario 6, which used a pure CART model.

Table 8 Extraction Result CART Gresik Regency

Classification CART	CART + MNDWI	CART MNDWI DEM

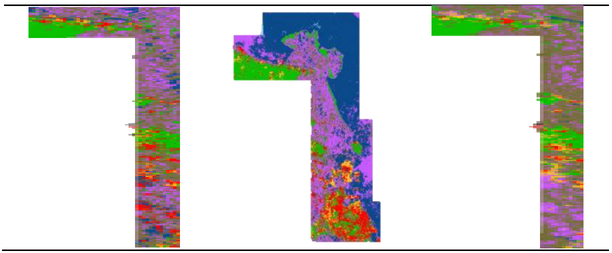

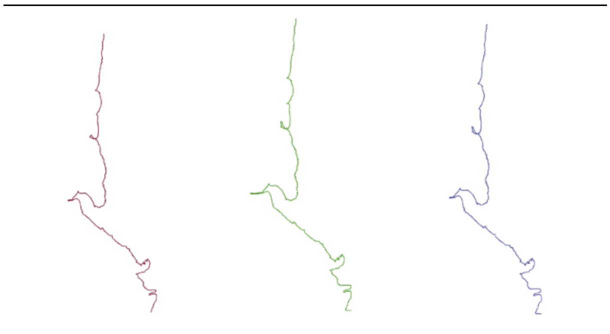

The results of the coastline extraction for Gresik Regency—specifically for Scenarios 6, 7, and 8 based on the OA—indicate that Scenario 6 is the best for Gresik Regency, as shown in Table 8. In the red square, the pure CART and MNDWI classifications produce a more realistic coastline compared to using the DEM, because in Ujungpangkah District, as previously noted, there are overestimated sections. Furthermore, in the red circle, the coastal industrial typology (JIIPE Port) can be seen using pure CART and DEM; however, since the DEM in Ujungpangkah Subdistrict is considered overestimated, pure CART can easily extract the coastline for typologies like those in Gresik Regency, which features diverse coastal typologies.

The results of the coastline extraction in Sidoarjo Regency for scenarios 6, 7, and 8 are shown in Table 9. The three coastline extraction scenarios are not significantly different; all three show the coastline, but the OA value for CART is lower than that for RF, which reaches 76%, while CART has the highest OA of 74% in scenario 8 (CART + MNDWI + DEM). This is comparable to the classification results, which show that river and sea water boundaries can still be distinguished, albeit only slightly.

Table 9. Extraction Result CART Sidoarjo Regency

Classification CART	CART + MNDWI	CART MNDWI DEM

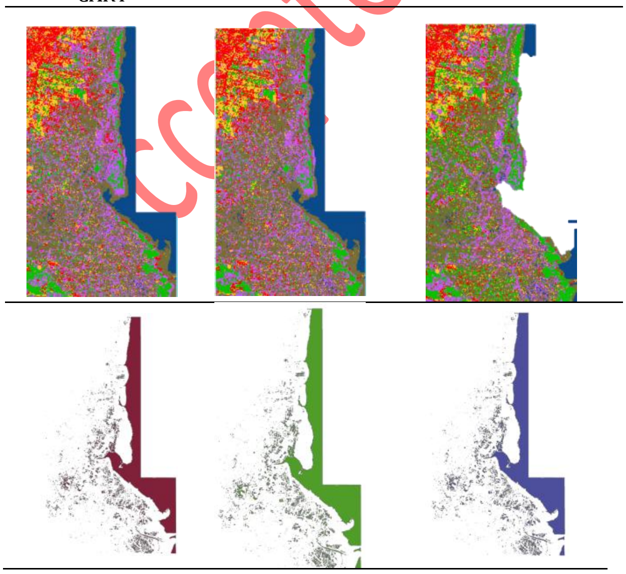

3.4 Result best Extraction

The performance of the machine learning algorithm exhibits contrasting characteristics in the two coastal study areas. The overall accuracy (OA) and Kappa coefficient for the Sidoarjo and Gresik areas are presented in Table 10.

In Sidoarjo Regency, the integration of MNDWI elevation data and RF machine learning (Scenario 5) successfully resolved the spectral confusion between seawater and inland ponds. Because the pond areas are physically located behind the embankments and have higher micro-elevations, the inclusion of DEM data prevented the RF model from misclassifying these artificial water bodies as open sea, thereby achieving a peak OA of 76%.

In contrast, in Gresik Regency, the pure CART model without additional indices or elevation data (Scenario 6) actually yielded the highest accuracy (OA = 66%, Kappa = 0.60). When the MNDWI and DEM variables were forced into the CART algorithm (Scenario 8), accuracy plummeted drastically to 48% (Kappa = 0.37). The splitting criteria in CART work by minimizing the Gini Impurity index on a single decision tree (Bayram et al., 2017).

Table 10. Result All Overall Accuracy (OA) and Kappa Coefficient

Scenario	Gresik		Sidoarjo	
	OA	KAPPA	OA (%)	KAPPA
3	0.59	0.51	72	0.66
4	0.63	0.55	72	0.66
5	0.63	0.55	**76**	**0.71**
6	**0.66**	**0.6**	68	0.62
7	0.62	0.55	72	0.66
8	0.48	0.37	74	0.68

Without an ensemble voting mechanism like that found in Random Forests, the single decision tree in CART is highly susceptible to overfitting when fed with multi-source data layers that are heavily noisy (Belgiu and Drăguţ, 2016). The 30-meter-resolution SRTM DEM has a vertical accuracy range of 10 to 16 meters. In the extremely flat floodplain zone along the Gresik coast, this coarse vertical resolution creates pseudo-microtopographic noise. The CART algorithm overfits to this vertical noise (Farda, 2017), leading to the formation of fragmented spatial decision boundaries and reducing the overall accuracy of the land cover map.

In contrast to the results of a previous study by (Arjasakusuma et al., 2021), which used the GMO Maximum Entropy (GMO-Maxent) statistical method, this study yielded more stable land-water classification results and higher accuracy (OA ranging from 84% to 95.2%) compared to Random Forest. The adaptation of the method to regional characteristics needs to be studied and adjusted so that the accuracy of the coastline extraction (Raychaudhuri et al., 2017), which will subsequently be used for DSAS, can more accurately map changes in the coastline (Khurram et al., 2025).

4. Conclusion

This study demonstrates that the accuracy of coastline extraction in tropical wetland areas is highly dependent on the compatibility between the choice of classifier algorithm and the physical typology of the coastline. Flat wetland areas dominated by regular ponds, such as in Sidoarjo, are best extracted using a Random Forest ensemble algorithm integrated with the MNDWI index and DEM topographic filters (OA = 76%). Conversely, industrial coastal areas with complex structures, such as in Gresik, are more accurately mapped using a pure CART model based on the image's native spectral channels (OA = 66%), to avoid classification bias caused by spatial noise from coarse elevation data.

Future research is expected to incorporate a wider variety of satellite imagery and the latest technologies, such as the use of SAR and high-resolution imagery. Spatial resolution remains a consideration, as pixel size can affect coastlines shifts of approximately 30 meters for Landsat imagery. However, this can be minimized by using high-resolution satellite imagery. Furthermore, distinguishing between river water, ponds, and open ocean water within wetland typologies presents a significant challenge for this study.

Acknowledgements

We would like to express our gratitude to Dr. Nurul Khakhim, M.Si., and Prof. Dr. Pramaditya Wicaksono, M.Sc., as our academic advisors, for their guidance, direction, and extraordinary patience throughout the preparation of this research. Without the assistance of all those involved, this article would not have been completed on time. High appreciation is also extended to Dr. Nur Mohammad Farda, S.Si., M.Cs., and Wirastuti Widyatmanti, S.Si., Ph.D., as the examination committee, for their corrections, feedback, and constructive scientific discussions in refining the classification methodology. The academic and administrative support from the Department of Remote Sensing, Graduate Program, Faculty of Geography, Gadjah Mada University was also instrumental in facilitating this study. Finally, the author thanks the United States Geological Survey (USGS) and NASA for providing Landsat imagery and SRTM DEM data, and Google Earth Engine for providing a reliable cloud computing platform. It is hoped that this research can be further developed regarding the optimization of coastline extraction in coastal areas with wetland typologies.

References

Adeli, A., Dastgheib, A., Roelvink, D., 2025. Shoreline dynamics prediction using machine learning models: from process learning to probabilistic forecasting. Front. Mar. Sci. 12. https://doi.org/10.3389/fmars.2025.1562504

Amukti, R., Adji, A.S., Ruslan, S., 2020. Analysis of Shoreline Shift using Satellite Imagery near Makassar City. Journal of Geoscience, Engineering, Environment, and Technology 5, 133–138. https://doi.org/10.25299/jgeet.2020.5.3.5111

Arifianto, I., Wibowo, R.C., 2020. Analysis of the Surface Subsidence of Porong and Surrounding Area, East Java, Indonesia based on Interferometric Satellite Aperture Radar (InSAR) Data. Journal of Geoscience, Engineering, Environment, and Technology 5, 199–205. https://doi.org/10.25299/jgeet.2020.5.4.5149

Arjasakusuma, S., Kusuma, S.S., Saringatin, S., Wicaksono, P., Mutaqin, B.W., Rafif, R., 2021. Shoreline dynamics in East Java Province, Indonesia, from 2000 to 2019 using multi-sensor remote sensing data. Land (Basel). 10, 1–17. https://doi.org/10.3390/land10020100

Aslam, R.W., Shu, H., Naz, I., Quddoos, A., Yaseen, A., Gulshad, K., Alarifi, S.S., 2024. Machine Learning-Based Wetland Vulnerability Assessment in the Sindh Province Ramsar Site Using Remote Sensing Data. Remote Sens. (Basel). 16. https://doi.org/10.3390/rs16050928

Barbier, E.B., Hacker, S.D., Kennedy, C., Koch, E.W., Stier, A.C., Silliman, B.R., 2011. The value of estuarine and coastal ecosystem services. Ecol. Monogr. https://doi.org/10.1890/10-1510.1

Bayram, B., Erdem, F., Akpinar, B., Ince, A.K., Bozkurt, S., Catal Reis, H., Seker, D.Z., 2017. THE EFFICIENCY OF RANDOM FOREST METHOD FOR SHORELINE EXTRACTION FROM LANDSAT-8 AND GOKTURK-2 IMAGERIES. ISPRS Annals of the Photogrammetry, Remote Sensing and Spatial Information Sciences IV-4/W4, 141–145. https://doi.org/10.5194/isprs-annals-IV-4-W4-141-2017

Belgiu, M., Drăguţ, L., 2016. Random forest in remote sensing: A review of applications and future directions. ISPRS Journal of Photogrammetry and Remote Sensing 114, 24–31. https://doi.org/10.1016/j.isprsjprs.2016.01.011

Çelik, O.İ., Gazioğlu, C., 2022. Coast type based accuracy assessment for coastline extraction from satellite image with machine learning classifiers. The Egyptian Journal of Remote Sensing and Space Science 25, 289–299. https://doi.org/10.1016/j.ejrs.2022.01.010

Congalton, R.G., Green, K., 2008. Assessing the Accuracy of Remotely Sensed Data. CRC Press. https://doi.org/10.1201/9781420055139

Costa Santos, C.S. da, Dias, F.F., Franz, B., Alves dos Santos, P.R., Fonseca Rodrigues, T. Da, Vargas, R., Américo dos Santos, C., 2019. RELATIVE SEA LEVEL RISE EFFECTS AT THE MARAMBAIA BARRIER ISLAND AND GUARATIBA MANGROVE: SEPETIBA BAY (SE BRAZIL). Journal of Sedimentary Environments 4, 249–262. https://doi.org/10.12957/jse.2019.44397

Eteh, D.R., Paaru, M., Egobueze, F.E., Okpobiri, O., 2024. Utilizing Machine Learning and DSAS to Analyze Historical Trends and Forecast Future Shoreline Changes Along the River Niger, Niger Delta. Water Conservation Science and Engineering 9. https://doi.org/10.1007/s41101-024-00324-1

Faiez, Z., Fan, D., 2023. Study of Coastal Morphological Changes by Tsunamis in Aceh (Indonesia) Using Satellite Images. Journal of Geoscience, Engineering, Environment, and Technology 8, 295–304. https://doi.org/10.25299/jgeet.2023.8.4.12757

Farda, N.M., 2017. Multi-temporal Land Use Mapping of Coastal Wetlands Area using Machine Learning in Google Earth Engine, in: IOP Conference Series: Earth and Environmental Science. Institute of Physics

Publishing. https://doi.org/10.1088/1755-1315/98/1/012042
Halim, 2016. Studying the changes of coastal line by applying remote sensing approach along the coastal Areas of Soropia Subdistrict 1, 24.
Hariyanto, T., Mukhtar, M.K., Pribadi, C.B., 2018. Evaluasi Perubahan Garis Pantai Akibat Abrasi Dengan Citra Satelit Multitemporal (Studi Kasus: Pesisir Kabupaten Gianyar, Bali). Geoid 14, 66. https://doi.org/10.12962/j24423998.v14i1.3822
Khurram, S., Pour, A.B., Bagheri, M., Helmy Ariffin, E., Akhir, M.F., Bahri Hamzah, S., 2025. Satellite-Based Multi-Decadal Shoreline Change Detection by Integrating Deep Learning with DSAS: Eastern and Southern Coastal Regions of Peninsular Malaysia. Remote Sens. (Basel). 17, 3334. https://doi.org/10.3390/rs17193334
Liang, Y., Zhang, J., Sun, W., Guo, Z., Li, S., 2025. Tracking the Construction Land Expansion and Its Dynamics of Ho Chi Minh City Metropolitan Area in Vietnam. Land (Basel). 14. https://doi.org/10.3390/land14061253
Li, K., Zhang, L., Chen, B., Zuo, J., Yang, F., Li, L., 2023. Analysis of China's Coastline Changes during 1990–2020. Remote Sens. (Basel). 15, 981. https://doi.org/10.3390/rs15040981
Lou, L., Chen, C., Li, M., Liu, K., 2024. Comparative Analysis of Water Body Extraction Accuracy Based on Thresholding Method. The International Archives of the Photogrammetry, Remote Sensing and Spatial Information Sciences XLVIII-4–2024, 331–336. https://doi.org/10.5194/isprs-archives-XLVIII-4-2024-331-2024
Marfai, M.A., Cahyadi, A., Anggraini, D.F., 2013. Typology, Dynamics, and Potential Disaster in The Coastal Area District Karst Gunungkidul. Forum Geografi 27, 147. https://doi.org/10.23917/forgeo.v27i2.2373
Mentaschi, L., Vousdoukas, M.I., Pekel, J.F., Voukouvalas, E., Feyen, L., 2018. Global long-term observations of coastal erosion and accretion. Sci. Rep. 8. https://doi.org/10.1038/s41598-018-30904-w
Muhammad Usman Zakaria, Wirastuti Widyatmanti, Retnadi Heru Jatmiko, 2025. Applied One-Dimensional Convolutional Neural Network Image Fusion Sentinel-1 SAR and Sentinel-2 for Classification and Mapping Dynamics of Coastal Wetlands in Segara Anakan, Cilacap Regency, Indonesia. Journal of Geoscience, Engineering, Environment, and Technology 10, 510–519. https://doi.org/10.25299/jgeet.2025.10.4.22909
Murray, N.J., Worthington, T.A., Bunting, P., Duce, S., Hagger, V., Lovelock, C.E., Lucas, R., Saunders, M.I., Sheaves, M., Spalding, M., Waltham, N.J., Lyons, M.B., 2022. High-resolution mapping of losses and gains of Earth's tidal wetlands. Science (1979). 376, 744–749. https://doi.org/10.1126/science.abm9583
Ondara, K., Dhiauddin, R., Wisha, U.J., Rahmawan, G.A., 2020. Hydrodynamics Features and Coastal Vulnerability of Sayung Sub-District, Demak, Central Java, Indonesia. Journal of Geoscience, Engineering, Environment, and Technology 5, 32–39. https://doi.org/10.25299/jgeet.2020.5.1.3996
Pattipawaej, O.C., Oktaviani, K., 2023. Analysis of shoreline changes in Yogyakarta coastal areas using remote sensing method, in: IOP Conference Series: Earth and Environmental Science. Institute of Physics. https://doi.org/10.1088/1755-1315/1134/1/012012
Raychaudhuri, K., Kumar, M., Bhanu, S., 2017. A Comparative Study and Performance Analysis of Classification Techniques: Support Vector Machine, Neural Networks and Decision Trees. pp. 13–21. https://doi.org/10.1007/978-981-10-5427-3_2
Sadewa, A.H., Supriyadi, A.A., 2024. The use of remote sensing in monitoring shoreline change: implications for maritime area security. Remote Sensing Technology in Defense and Environment 1, 28–35. https://doi.org/10.61511/rstde.v1i1.2024.841
Simarmata, N., Adlan Nadzir, Z., Nawang Sari, D., Terusan Ryacudu, J., Way Hui, D., Jatiagung, K., Selatan, L., n.d. Analisis Perubahan Garis Pantai Menggunakan Metode Sentinel-1 Dual-Polarized Water Index ANALISIS PERUBAHAN GARIS PANTAI MENGGUNAKAN METODE SENTINEL-1 DUAL-POLARIZED WATER INDEX (SDWI) BERBASIS DATA MULTITEMPORAL PADA GOOGLE EARTH ENGINE (Shoreline Change Analysis with Sentinel-1 Dual-Polarized Water Index (SDWI) Method based on Multitemporal Data using Google Earth Engine).
Syamani 2021 Comparison of Various Spectral Indices for Optimum Extraction of Tropical Wetlands Using Landsat 8 OLI, n.d.
Tyralis, H., Papacharalampous, G., Langousis, A., 2019. A Brief Review of Random Forests for Water Scientists and Practitioners and Their Recent History in Water Resources. Water (Basel). 11, 910. https://doi.org/10.3390/w11050910
Xu, H., 2006. Modification of normalised difference water index (NDWI) to enhance open water features in remotely sensed imagery. Int. J. Remote Sens. 27, 3025–3033. https://doi.org/10.1080/01431160600589179